Optimal Sizing, Energy Balance, Load Management and Performance Analysis of a Hybrid Renewable Energy System

Kelvin Nkalo Ukoima [1,*] , **Ogbonnaya Inya Okoro** [1] , **Patrick Ifeanyi Obi** [1] , **Udochukwu Bola Akuru** [2] and **Innocent Ewean Davidson** [3]

1   Department of Electrical Electronic Engineering, Michael Okpara University of Agriculture, Umudike 440101, Nigeria
2   Department of Electrical Engineering, Tshwanne University of Technology, Pretoria 0001, South Africa
3   Department of Electrical Electronic and Computer Engineering, French-South African Institute of Technology (F'SATI)/African Space Innovation Centre (ASIC), Cape Peninsula University of Technology, Bellville 7535, South Africa
*   Correspondence: kelvin.ukoima@mouau.edu.ng

Abstract: This work utilizes the particle swarm optimization (PSO) for optimal sizing of a solar–wind–battery hybrid renewable energy system (HRES) for a rural community in Rivers State, Nigeria (Okorobo-Ile Town). The objective is to minimize the total economic cost (TEC), the total annual system cost (TAC) and the levelized cost of energy (LCOE). A two-step approach is used. The algorithm first determines the optimal number of solar panels and wind turbines. Based on the results obtained in the first step, the optimal number of batteries and inverters is computed. The overall results obtained are then compared with results from the Non-dominant Sorting Genetic Algorithm II (NGSA-II), hybrid genetic algorithm–particle swarm optimization (GA-PSO) and the proprietary derivative-free optimization algorithm. An energy management system monitors the energy balance and ensures that the load management is adequate using the battery state of charge as a control strategy. Results obtained showed that the optimal configuration consists of solar panels (151), wind turbine (3), inverter (122) and batteries (31). This results in a minimized TEC, TAC and LCOE of USD 469,200, USD 297,100 and 0.007/kWh, respectively. The optimal configuration when simulated under various climatic scenarios was able to meet the energy needs of the community irrespective of ambient conditions.

Keywords: feasibility; hybrid; power; homer; solar; wind

1. Introduction

The global energy landscape is undergoing a significant transformation driven by the main goal of reducing greenhouse gas emissions and ensuring energy security. A promising solution to this is the deployment of Hybrid Renewable Energy Systems (HRESs). These systems combine multiple sources of renewable energy, such as solar, wind, and hydro, to provide a reliable and sustainable power supply.

As of September 2023, Nigeria's electricity production reached 8415 GWh [1]. However, the country's national electricity grid has been unstable, with more than 200 collapses in the last nine years, often leading to widespread blackouts, with the national rate of electricity access being just 58% [1]. The extension of the grid to rural areas is often unfeasible due to factors such as challenging terrains, remote locations, high supply costs, low consumption rates, low household incomes, poor road infrastructure, and scattered consumer settlements. As a result, many rural inhabitants depend on alternative sources like diesel generators for their electricity needs. However, this solution comes with its own set of problems, including noise pollution, greenhouse gas emissions, and high maintenance and fuel costs. In response to increasing environmental concerns, there is a push for the Nigerian electrical power industry to turn to cleaner sources for electricity generation. These sources,

which include wind, solar, biomass, small hydro, and geothermal, are locally available, environmentally friendly, free, and unlimited. However, the intermittent nature of RE sources, which often necessitates system oversizing and the use of large energy storage devices, can lead to substantial investment costs.

In terms of HRES sizing, numerous studies have been conducted over the years. Agajie et al. [2] investigated the optimal design and mathematical modeling of a hybrid solar PV–biogas generator system with energy storage. Their study focused on multi-objective function cases to enhance the system's economic viability, reliability, and environmental impact. Adewuyi et al. [3] explored a multi-objective mix generation planning approach considering utility-scale solar PV systems and voltage stability, specifically for Nigeria, highlighting the importance of integrating solar PV to improve voltage stability and overall system reliability. Al-Masri et al. [4] developed an optimal energy management strategy for a hybrid photovoltaic–biogas energy system using multi-objective grey wolf optimization. They aimed to optimize the system's performance and cost-effectiveness. Xu et al. [5] proposed an improved optimal sizing method for wind–solar–battery hybrid power systems, focusing on enhancing the reliability and efficiency of hybrid systems through better sizing strategies. Al-Masri et al. [6] examined the impact of different photovoltaic models on the design of a combined solar array and pumped hydro storage system with the aim of optimizing the system's performance and cost-effectiveness. Similar studies also utilize conventional strategies (like analytical, numerical, iterative, and probabilistic methods) [7–10]. Artificial intelligence techniques like Grey Wolf Optimization (GWO), PSO, Cuckoo Search Algorithm (CSA), GA, Ant Colony Optimization (ACO), and Artificial Bee Colony (ABC) have also been explored. For instance, Al-Masri et al. [11] explored the optimal allocation of a hybrid photovoltaic–biogas energy system using multi-objective feasibility-enhanced particle swarm algorithm. They focus on improving system reliability and cost-effectiveness. Sultan et al. [12] introduced an improved artificial ecosystem optimization algorithm for the optimal configuration of a hybrid PV/WT/FC energy system. It aims to enhance system performance and efficiency. Ukoima et al. [13] presented a modified multi-objective particle swarm optimization (m-MOPSO) for the optimal sizing of a solar–wind–battery hybrid renewable energy system with a focus on improving the system's efficiency and reliability. Diab et al. [14] explored the sizing of a hybrid solar/wind/hydroelectric pumped storage energy system in Egypt using different meta-heuristic techniques with the aim of enhancing system performance and cost-effectiveness. Alotaibi et al. [15] designed a smart strategy for sizing a hybrid renewable energy system to supply remote loads in Saudi Arabia focusing on optimizing system performance and cost-effectiveness. Iturki and Awawad [16] minimized costs of a standalone hybrid wind/PV/biomass/pump-hydro storage-based energy system with the aim of enhancing the system performance and reducing the cost. Other studies also explored AI techniques for optimal sizing [17–21]. Furthermore, hybrid methods like GA-PSO, Simulated Annealing–Tabulated Search, and GA-ABC are also the focus of recent studies. For example, Fadli and Purwoharjono [22] investigated optimal sizing of a PV/diesel/battery hybrid microgrid using a multi-objective bat algorithm. Shi et al. [23] addressed size optimization of stand-alone PV/wind/diesel hybrid power generation systems. Javed and Ma [24] conducted a techno-economic assessment of a hybrid solar–wind–battery system using a GA-ABC algorithm, focusing on optimizing system performance and cost-effectiveness. Emad et al. [25] explored the techno-economic design of a hybrid PV/wind system with battery energy storage for a remote area. Hatata et al. [26] proposed an optimization method for sizing a solar/wind/battery hybrid power system based on the artificial immune system with a focus on improving system performance and cost-effectiveness. Askarzadeh and Coelho [27] introduced a novel framework for optimizing grid-independent hybrid renewable energy systems, focusing on a case study in Iran. Li et al. [28] presented the optimal design and techno-economic analysis of a solar–wind–biomass off-grid hybrid power system for remote rural electrification in West China. They aim to improve system reliability and cost-effectiveness. Goswami et al. [29] developed a grid-connected solar–wind hybrid system with reduced levelized tariff for

a remote island in India. The utilization of computer software like HOMER, Transient System Simulation Tool and General Algebraic Modeling System is also in the limelight. Aziz et al. [30] investigated the optimal sizing of standalone hybrid energy systems for rural electrification in Iraq. They considered sensitivity analysis to enhance system performance and reliability. Kumar and Channi [31] designed a PV–biomass off-grid hybrid renewable energy system (HRES) for rural electrification. They analyzed techno-economic and environmental aspects of the proposed system. Hashem et al. [32] explored optimal placement and sizing of wind turbine generators and superconducting magnetic energy storage in a distribution system. They aimed to improve system efficiency and reliability. Duchaud et al. [33] investigated multi-objective particle swarm optimization for sizing a renewable hybrid power plant with storage. They addressed factors such as cost, reliability, and environmental impact. Rezk et al. [34] sized a stand-alone hybrid PV–fuel cell–battery system for desalinating seawater at Saudi NEOM City. They considered energy sustainability and water production. Donado et al. [35] developed a multi-objective optimization tool for configuring renewable hybrid energy systems. They explored various energy sources and system configurations. Generally, these studies use a variety of indicators to evaluate HRES performance. These indicators can be economic (levelized cost of energy, net present cost, total annualized cost, reliability-based (loss of power supply probability (LPSP) and loss of load probability), environmental (like life cycle assessment, life cycle emission and carbon footprint of energy), or social (social acceptance, job creation index, human development index).

From the reviewed literature, most of the research papers focused solely on system sizing or energy control. A successful energy management system must be combined with a suitable sizing method. The aim of this study is to develop a comprehensive approach to the operation of HRES, integrating optimal sizing, energy balance, load management, and control strategy. The optimal sizing of HRES is crucial to ensure that the system can meet the energy demand at the lowest possible cost. Energy balance involves managing the supply and demand of energy within the system, ensuring that energy production matches consumption. Load management strategies are used to control and optimize the operation of the HRES, improving its efficiency and reliability. Finally, the control strategy is essential for the stable and efficient operation of the HRES, managing the interaction between different energy sources and the load. Optimal sizing, energy balance, load management and control are separate but interconnected facets of the same Hybrid Renewable Energy System (HRES). A system that is optimally sized but lacks energy balance, load management and control will not operate efficiently.

Our optimal sizing model identifies the least costly structure of the HRES. The model is then combined with an Energy Management System (EMS) algorithm, which guarantees optimal energy scheduling during system operation. The combination of these two systems will result in a mutual model that guarantees energy reliance at the lowest possible cost. This study employs PSO to achieve this. It is a widely recognized optimization algorithm that stands out due to its numerous benefits compared to other similar algorithms. Its advantages encompass its simplicity, the fact that it does not require derivatives, its use of a limited number of parameters, which eases the tuning process, its ability to be easily parallelized, and its insensitivity to scaling, meaning that the performance of PSO remains largely unaffected by the scaling of design variables. The performance of the PSO is then compared with results obtained from the hybrid GA-PSO, NGSA-II, and proprietary derivative-free optimization algorithms.

This study contributes the following:

1. Development of a comprehensive HRES optimization model that integrates optimal sizing, energy balance, load management, and control strategy into a single model. This model ensures that the system can meet the energy demand at the lowest possible cost while maintaining efficiency and reliability.
2. Utilization of the PSO for optimal sizing of a solar–wind–battery hybrid renewable energy system (HRES) and comparing the performance of PSO with hybrid GA-

PSO, NGSA-II, and proprietary derivative-free optimization algorithms, providing a detailed analysis of the trade-offs between cost and performance for different optimization methods.

3. Evaluation of the economic indicators (TEC, TAC, LCOE) and performance metrics (reliability) of the proposed HRES configurations.

The limitation of this study is the following:

1. The study does not consider the detailed electrical network model. Hence, this study does not consider issues related to voltage stability, power quality, inverter power and network losses.

The remainder of this paper is structured as follows. Section 2 outlines the materials and methods, Section 3 presents the results and discussion, and Section 4 concludes the paper.

2. Materials and Methods

Matlab 2020a and HOMER v3.16.2 were used in running the simulations. Firstly, the PSO was used to find the optimal number of solar panels and wind turbines. The results obtained are then used to compute the number of batteries and inverters required. The overall results are then compared with results obtained from the hybrid GA—PSO, NGSA-II and proprietary derivative-free optimization algorithm. Finally, the optimal configurations are then simulated under various weather conditions to evaluate the general performance under varying conditions. The research framework is shown in Figure 1.
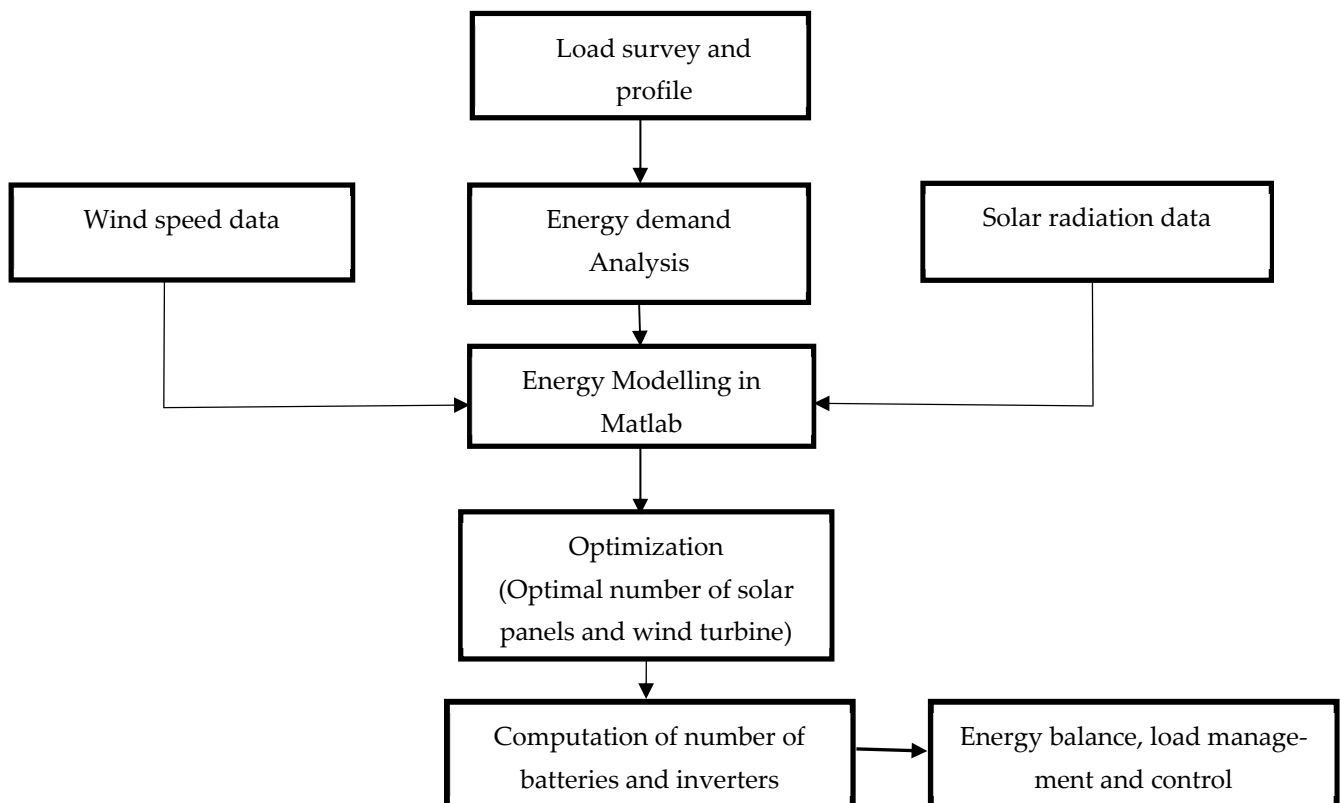

Figure 1. Research framework.

2.1. Description of Okorobo-Ile Town and Load Profile

Okorobo-Ile is a remote village situated in the South-South region of Nigeria, at the boundary between the Rivers and Akwa-Ibom States. The village has a population of about 6,700 people, spread across approximately 600 households. It includes essential community facilities such as schools, churches, and a town hall. Most residents leave their homes

in the morning and return in the evening. The community's total daily energy demand (TED) is 656.36 kWh, with a peak load of 99.12 kW and a total daily load of 678 kW. A comprehensive technical analysis of the community's load demand and profile is available in [36]. Figure 2 illustrates the community's load profile.
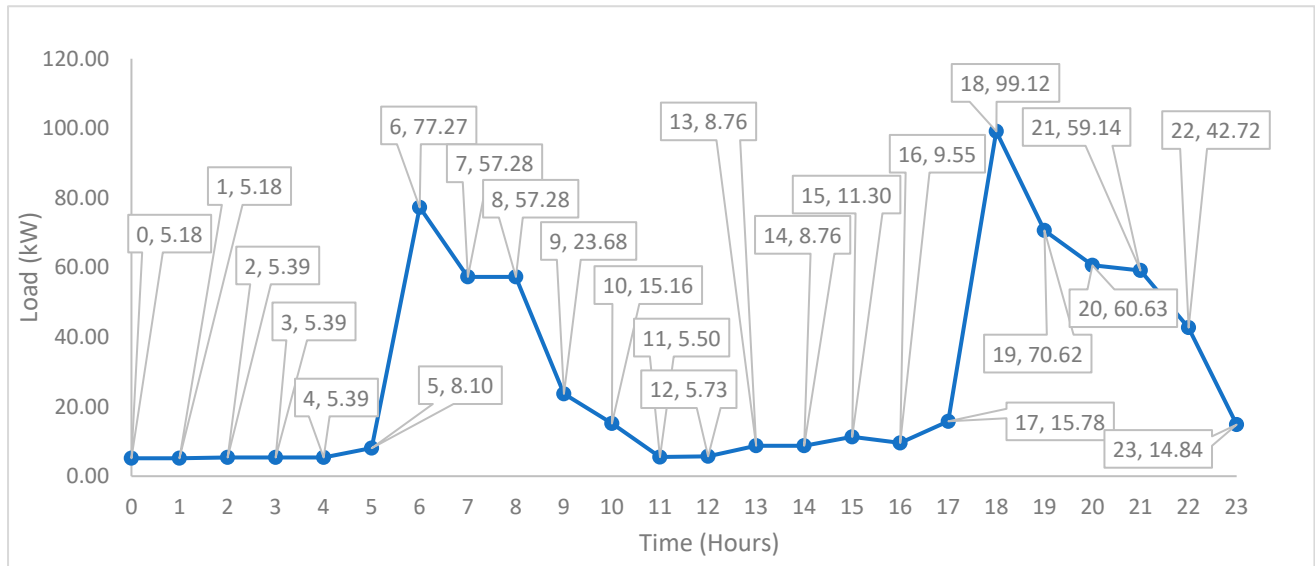

Figure 2. Detailed load profile of Okorobo-Ile town [36,37].

2.2. Resource Data

The solar data for the site were sourced from the NASA solar energy radiation database, as depicted in Figure 3. Wind speed data were collected through hourly measurements from January 2020 to January 2023 using a UNI-T Bluetooth digital anemometer installed at a height of 10 m. Figure 4 illustrates the wind speed plot for the site.
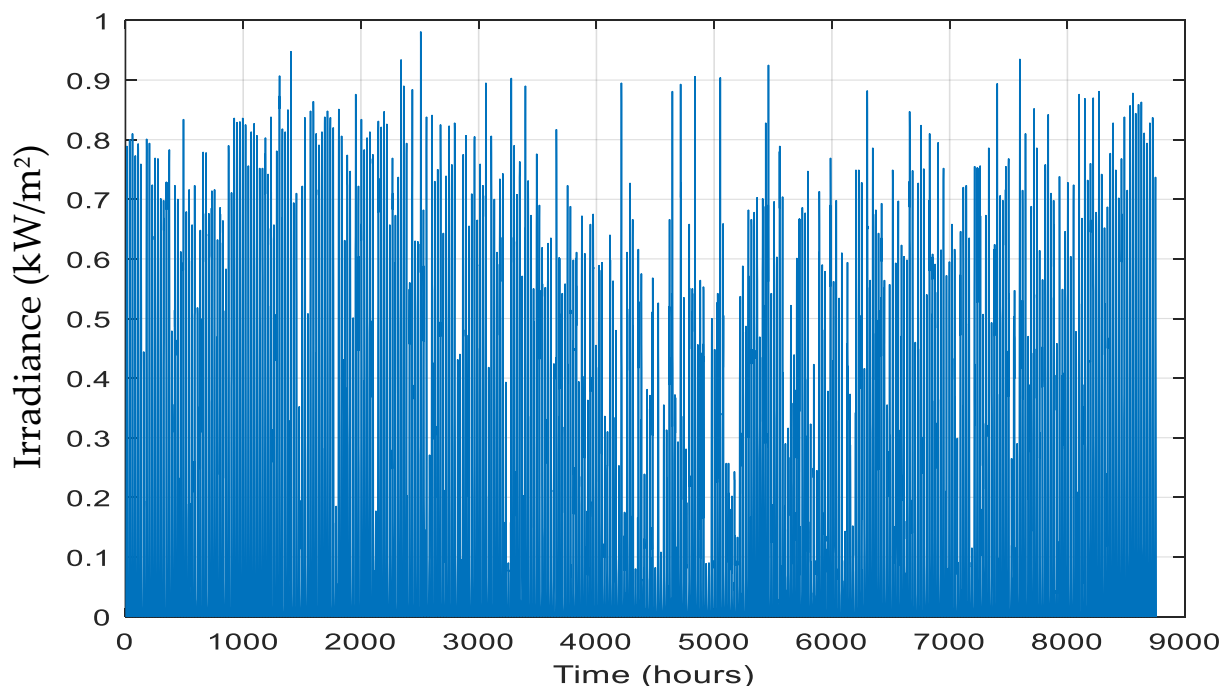

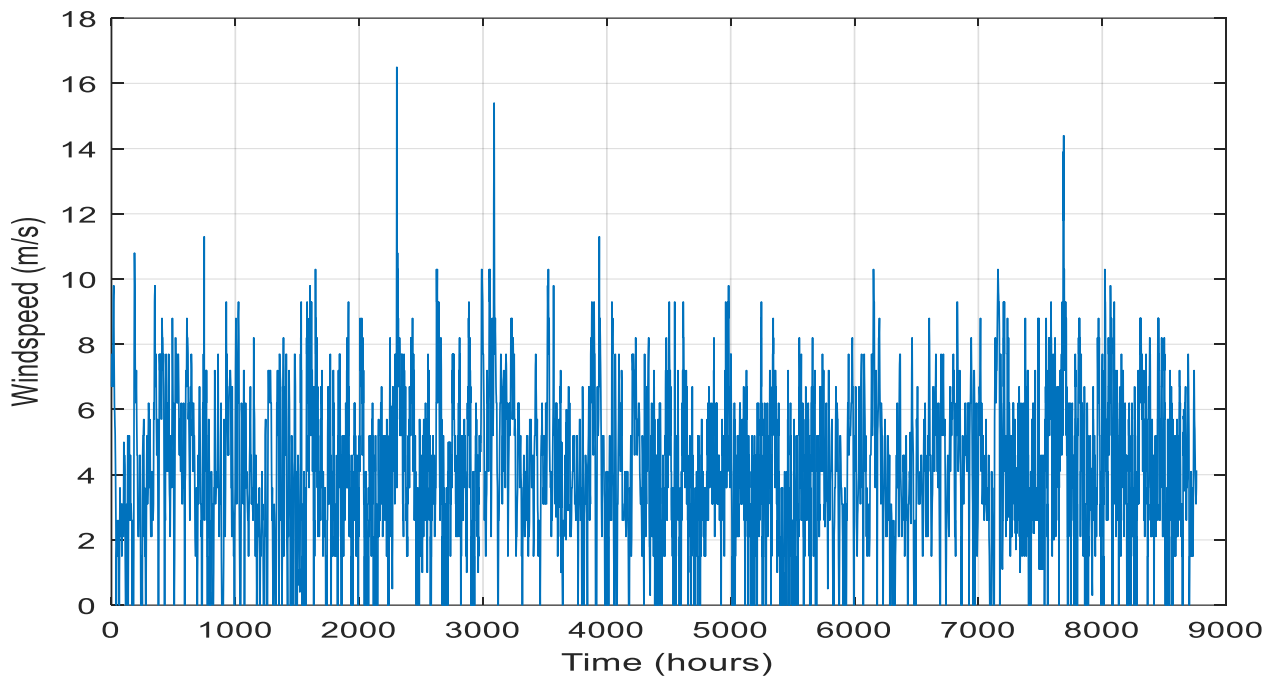**Figure 3.** Solar irradiance hourly profile.

Figure 4. Wind speed hourly profile at 10 m height.

2.3. Mathematical Model of the HRES

2.3.1. PV Panels

The hourly output power of a PV module is defined as [38,39]:

$$P_{pv}(t) = G(t) \times A \times \eta \tag{1}$$

G(t) represents the hourly solar irradiance at the site, as shown in Figure 1. The area of the panel is denoted by (A) (1 m^2), and (η) is the solar panel efficiency (20%). In this study, it is assumed that the PV modules are equipped with a maximum power point tracking (MPPT) system, and temperature effects are disregarded. If (x(1)) is the number of PV modules to be optimized, the total PV power can be calculated as follows:

$$P_{pv} = x(1)P_{pv} \tag{2}$$

2.3.2. Wind Turbine

Several formulas exist for the power output of a wind turbine. In this study, we use the following formula:

$$P_w(v) = \begin{cases} 0 & v \leq v_c \& v \geq v_f \\ P_r \times \frac{v^3 - v_c^3}{v_r^3 - v_c^3} & v_c \leq v \leq v_r \\ P_r & v_r \leq v \leq v_f \end{cases} \tag{3}$$

In this study, (v) represents the wind speed at the wind turbine's hub. (V_c) is the cut-in speed, (V_r) is the rated speed, and (V_f) is the cutoff speed. The wind turbine has a rating of 25 kW, with a rated speed of 3 m/s and a cut-in speed of 2 m/s. The conversion of the measured wind speed at a given height to the turbine hub speed is performed using the power law.

$$v = v_{measure} \times \left(\frac{h_{hub}}{h_{measure}} \right)^{\alpha} \tag{4}$$

The exponent law coefficient, (α), varies depending on factors such as the season, nature of the terrain, time of day, elevation, temperature, wind speed, and various thermal and mechanical mixing parameters. When specific site data are unavailable, (α) is typically

assumed to be 0.14, while for windy locations, (α) is taken as 0.25. If (x(2)) represents the number of wind turbines to be optimized, the total wind power can be calculated as follows:

$$P_w = x(2)P_w \tag{5}$$

2.3.3. Number of Inverters

In this study, the calculation of the number of inverters is primarily based on the peak load. This is because the inverter must be capable of handling the highest power demand the system will encounter at any given time to prevent overloading. To account for potential future system expansion, a small margin above the calculated peak load is included to ensure reliability. The algorithm follows these steps to compute the number of inverters:

Determine the HRES peak power.

Determine the peak load from the load profile.

Compare the peak load from the load profile with the peak power generated by the HRES. The higher value is considered the peak power.

Add a safety margin of 23% for reliability and future load expansion.

Assuming each inverter has a rating of 1 kW and an efficiency of 95%, the number of inverters, (x(3)), is calculated as follows:

$$x(3) = \frac{peak\_power}{inverterrating \times inverterefficiency} \tag{6}$$

2.3.4. Number of Batteries

The energy generated by the HRES can be used to meet the community's needs during production hours. Any surplus energy can be stored in batteries for use when renewable sources are not generating power, such as at night or during low-wind periods.

The following steps are used by the algorithm to compute the number of inverters.

Determine the daily energy generated by the HRES.

Energy storage required = daily energy demand − daily energy generated.

Add a safety margin of 23% for reliability and future load expansion.

Assuming that the rating of one battery is 72 kW, dod is 80%, inverter efficiency is 90%, 0.85 is battery efficiency, and 23% is the safety factor, then the number of batteries, x(4), is given as:

$$x(4) = \frac{(dailyenergygenerated - dailyenergydemand)}{safetyfactor \times dod \times batterycapacityxbatteryefficiency \times inverterefficiency} \tag{7}$$

2.4. Optimization Problem Formulation

2.4.1. Decision Variables

In this study, the considered decision variables are:

Number of PV panels—x(1);

Number of wind turbines—x(2);

Number of inverters—x(3);

Number of batteries—x(4).

2.4.2. Objective Function

The objective of this study is to minimize the total economic cost (TEC) of the HRES. The TEC is defined as:

$$TEC_{(x(1),x(2),x(3),x(4))} = TAC + TC + I\_C - SV \tag{8}$$

(TAC) is the Total Annual Cost;

(TC) is the Tax Cost;

(I_C) is the Insurance Cost;

(SV) is the Salvage Value.

The Total Annual Cost is given by:

$$\text{TAC} = C\_C + C\_OM + C\_R \tag{9}$$

C_C is the annualized capital cost;

C_OM is the operation and maintenance cost;

C_R is the annualized replacement cost.

The annualized capital cost is calculated as:

$$C\_C = IC \times CRF \tag{10}$$

(IC) is the Total Initial Cost;

(CRF) is the Capital Recovery Factor.

The total initial cost IC is given by:

$$
\begin{aligned}
IC = x(1). \text{ Capital cost per solar panel} + x(2). \text{ Capital cost per wind turbine} + \\
x(3). \text{ Capital cost per inverter} + x(4). \text{ Capital cost per battery.}
\end{aligned} \tag{11}
$$

The capital recovery factor, CRF is defined as:

$$CRF = \frac{\text{discountrate} \times (1 + \text{discountrate})^{\text{projectlife}}}{(1 + \text{discountrate})^{\text{projectlife}-1}} \tag{12}$$

(r) is the discount rate;

(n) is the project life.

The operation and maintenance cost (C_OM) is given by:

$$
\begin{aligned}
C\_OM = x(1). \text{ Operation maintenance cost per solar panel} + x(2). \\
\text{Operation maintenance cost per wind turbine} + x(3). \\
\text{Operation and maintenance cost per inverter} + x(4). \\
\text{Operation maintenance cost per battery}
\end{aligned} \tag{13}
$$

The annual operation and maintenance cost does not include the capital recovery factor. It is generally considered a fixed cost associated with the operation and maintenance of the system.

The annualized replacement cost (C_R) is given by:

$$C\_R = RC \times CRF' \tag{14}$$

(RC) is the Replacement Cost;

(CRF') is the modified Capital Recovery Factor.

The replacement cost (RC) is given by:

$$
\begin{aligned}
RC = x(1). \text{ Replacement cost per solar panel} + x(2). \\
\text{replacement cost per wind turbine} + x(3). \\
\text{replacement\_cost\_inverter} + x(4). \text{ replacement cost per battery}
\end{aligned} \tag{15}
$$

The modified capital recovery factor is defined as:

$$CRF' = \frac{\text{discountrate} \times (1 + \text{discountrate})^{\frac{\text{projectlife}}{2}}}{(1 + \text{discountrate})^{\frac{\text{projectlife}}{2}-1}} \tag{16}$$

This assumes that the project components need to be replaced halfway through the project life.

The annualized tax cost is given as:

$$TC = \text{tax rate} \times (IC - SV) \tag{17}$$

A tax rate of 30% is used in this study.

The salvage value (SV) at the end of the project life is given as:

$$SV = \frac{0.2 \times IC}{(1 + \text{discountrate})^{\text{projectlife}}} \tag{18}$$

This assumes that salvage value is 20% of component cost.

I_C is the annual insurance cost and is given as:

$$I\_C = \text{insurance rate} \times IC \tag{19}$$

An insurance rate of 5% is used in this study.

2.4.3. Constraint

The constraint used in this study is given below.

The first constraint is as follows: $X_{kmin} \leq X_k \leq X_{kmax}$, k ϵ [PV panels, wind turbines].
X_k = integer, k ϵ [PV panels, wind turbines]

This constraint defines the minimum and maximum limits for the number of solar panels and wind turbines to minimize land costs. In this study, the maximum number of solar panels and wind turbines was set at 165 and 3, respectively, while the minimum was set at 50 and 0, respectively.

The second constraint is as follows: Daily power generated $\geq$ daily load profile.

2.4.4. Technique for Optimization

This study uses Particle Swarm Optimization (PSO), which is an algorithm inspired by the social behavior of species like birds or fish that move in groups to reach a shared objective. It is an algorithm that falls under the domain of swarm intelligence, which is a subset of artificial intelligence. In the context of PSO, a swarm of particles, each symbolizing a potential solution, explores the solution space of a problem to identify the most optimal solution. The movement of each particle is dictated by its own best-known position and is also steered towards the best-known positions in the search space, which are updated as other particles discover better positions. This heuristic method is designed to guide the swarm towards the most optimal solutions. This is shown in Figure 5. The result of the optimization technique is then compared with the hybrid GA-PSO, NGSA-II and the proprietary derivative-free algorithm used in HOMER. The hybrid GA-PSO algorithm leverages the strengths of both the genetic algorithm (GA) and Particle Swarm Optimization (PSO). By initializing the GA with data from the PSO, the GA starts with a strong foundation, helping it to avoid local optima and enhance its search efficiency.

2.5. Energy Balance, Control and Load Management

For energy balance, the algorithm calculates the energy balance at each time step by subtracting the load (energy demand) from the total DC power generated by the wind and solar sources. This balance determines whether there is excess or insufficient generation. If there is excess generation, the surplus energy is stored in the battery. If there is insufficient generation, energy is drawn from the battery. This process ensures that the energy produced matches the energy consumed, thus maintaining a balance. The battery state of charge control part of the algorithm monitors the state of charge (SOC) of the battery based on the energy balance. If there is excess generation, the battery is charged up to its capacity. If there is insufficient generation, the battery is discharged, but not below a minimum SOC. This control mechanism ensures that the battery is used optimally, prolonging its life and ensuring that it can provide power when needed. In the load management section, if there

is still a remaining load after accounting for the total DC power and the battery, the diesel generator is used. The amount of generation from the diesel generator is controlled to meet the remaining load, but within the generator's capacity and minimum load. This ensures that the load is met at all times. The diesel generator was included in the algorithm to see if it is possibly needed. The diesel generator control controls the diesel generator's operation to prevent rapid changes in its output. This is performed by limiting the ramp rate, which is the change in generation from one time step to the next. This control mechanism can prevent potential damage to the generator due to rapid changes in load.
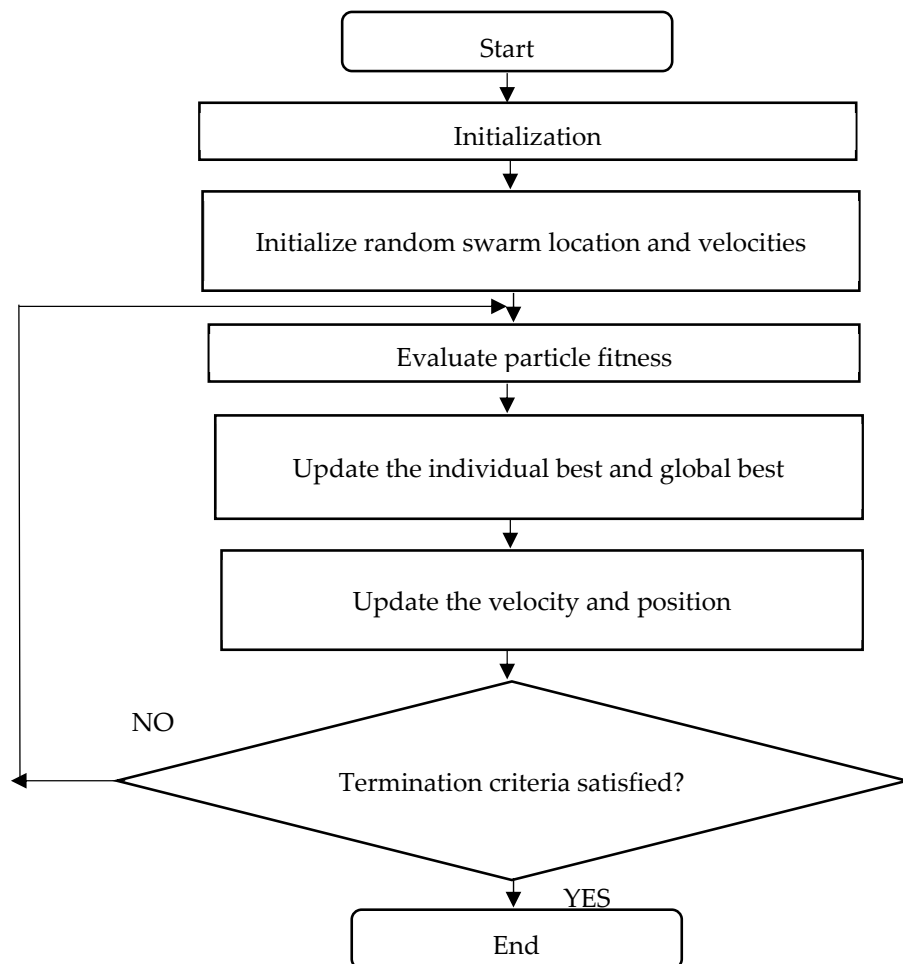
Figure 5. Flow chart of the PSO optimization process.

The energy balance, control and load management are achieved with the following steps:

1. **Calculate total DC power**: This is calculated by adding the power output from the WT and PV panels.
2. **Calculate the energy balance (E_b):** This is calculated by subtracting the load profile (the energy demand at time i) from the total DC power.
3. **Update battery state of charge (SOC):** Depending on the energy balance, the battery SOC is updated as follows.

If there is excess generation (Energy_balance > 0), the energy is stored in the battery. The amount of energy stored is limited by the battery's power rating and charging efficiency. The SOC is also limited to the battery's capacity.

If there is insufficient generation (Energy_balance < 0), energy is drawn from the battery. The amount of energy drawn is limited by the battery's power rating and discharging efficiency. The SOC is also limited to a minimum SOC.

If the energy balance is zero, the battery SOC remains unchanged.

4. **Calculate remaining load:** The remaining load is calculated by subtracting the total DC power and the change in battery SOC from the load profile.
5. **Possible diesel generator operation**: If there is a remaining load, the diesel generator is used. The amount of generation is limited by the generator's capacity and its minimum load. The generator's ramp rate is also taken into account to limit the change in generation from one time step to the next.

2.6. Technical Specifications for Optimization

The optimization algorithm minimizes the TAC while ensuring that the solution is adequate in meeting the community's energy demand. The selection process considers the type, rating, and pricing of the Hybrid Renewable Energy Systems (HRESs). The technical specifications are detailed in Table 1.

Table 1. Technical specifications for optimization.

Solar Panel	Specification
Max power	1 kW
Dimension	1.8×1.0 m
Panel efficiency	19.3%
Panel temperature coefficient	$-0.005/^{\circ}$C
Initial cost (IC)	USD 1200/kW
O & M cost	USD 10/kW
Replacement cost	USD 1000/kW
Life span	20 years
Wind turbine	
Rated power	25 kW
Cutin speed	5 m/s
Rated speed	12 m/s
Cutoff speed	25 m/s
Initial cost	USD 5000/kW
O & M cost	USD 500/kW
Replacement cost	USD 5000/kW
Life span	20 years
Inverter	
Rating	1 kW
Efficiency	95%
Battery	
Rating	72 kWh
Depth of Discharge (dod)	80%
Efficiency	85%
Economic	
Inflation rate	40%
Discount rate	30%
Tax rate	30%
Insurance rate	5%
Salvage	20% of IC

3. Results and Discussion

3.1. Result from Particle Swarm Optimization

The optimal configuration is composed of 154 PV modules, three wind turbines, 136 inverters and 31 batteries. Figure 6 shows the power generated from the optimal configuration. The annual electrical energy produced by the system was 42.17 MWh, of which 41.974 MWh is solar PV, and 196.59 kWh is from wind turbine. The minimized

total economic cost (TEC) and the total annual cost are USD 476,731 and USD 301,947, respectively. This results in an LCOE of 0.011 USD/kWh. The other cost associated with the TEC was USD 174,784. The total operation and maintenance cost, total replacement cost and total capital cost of the optimal system were found to be USD 219,772, USD 446,300 and USD 341,630, respectively. Figure 7 shows the optimized fitness function and Figure 8 shows a breakdown of the capital cost. The PV and wind turbine represented 37% and 30% of the capital cost of the system, respectively. The number of wind turbines was limited to a maximum of three (3) in the algorithm as a result of its high cost. Therefore, solar PV and wind turbines are the critical components in the stand-alone HRES for the region. The battery bank's cost makes up 25% of the total capital cost, while the inverter cost accounts for about 8%.
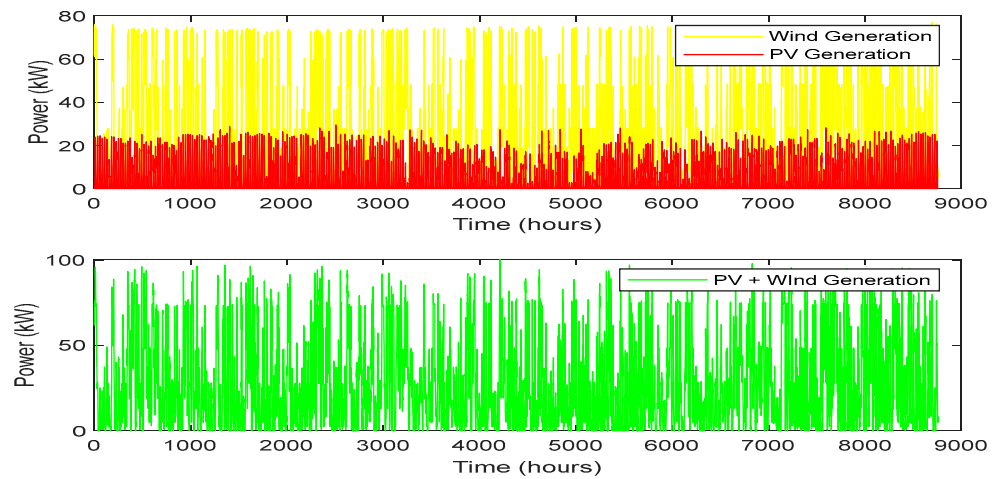
Figure 6. Power generated from the HRES.
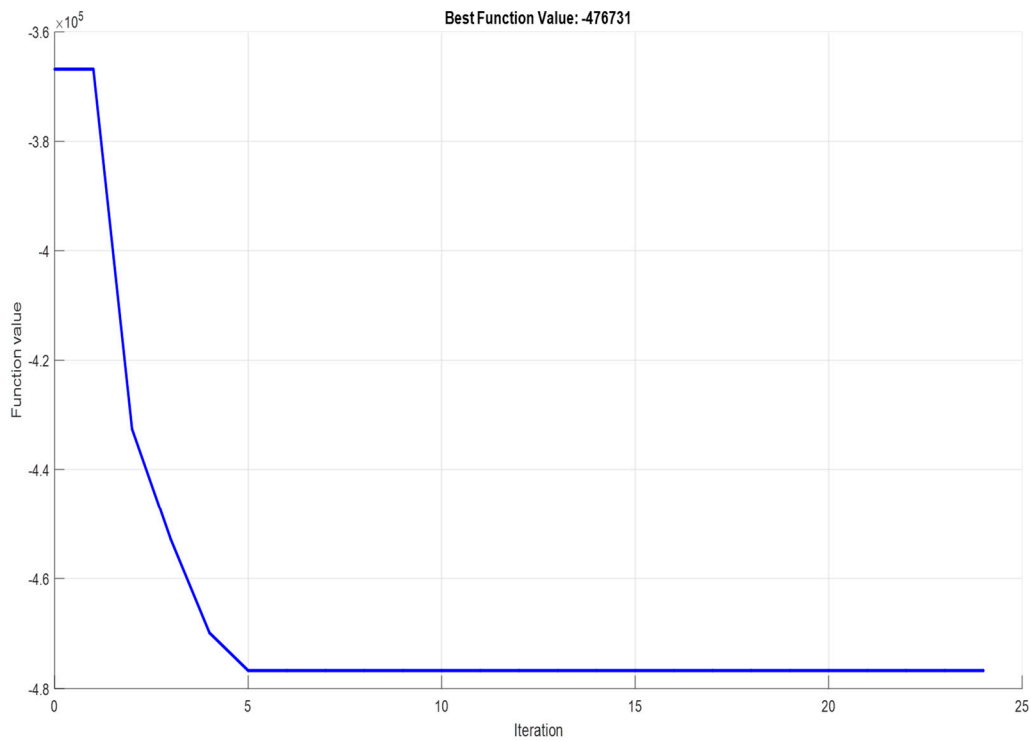
Figure 7. Optimized fitness function from PSO.
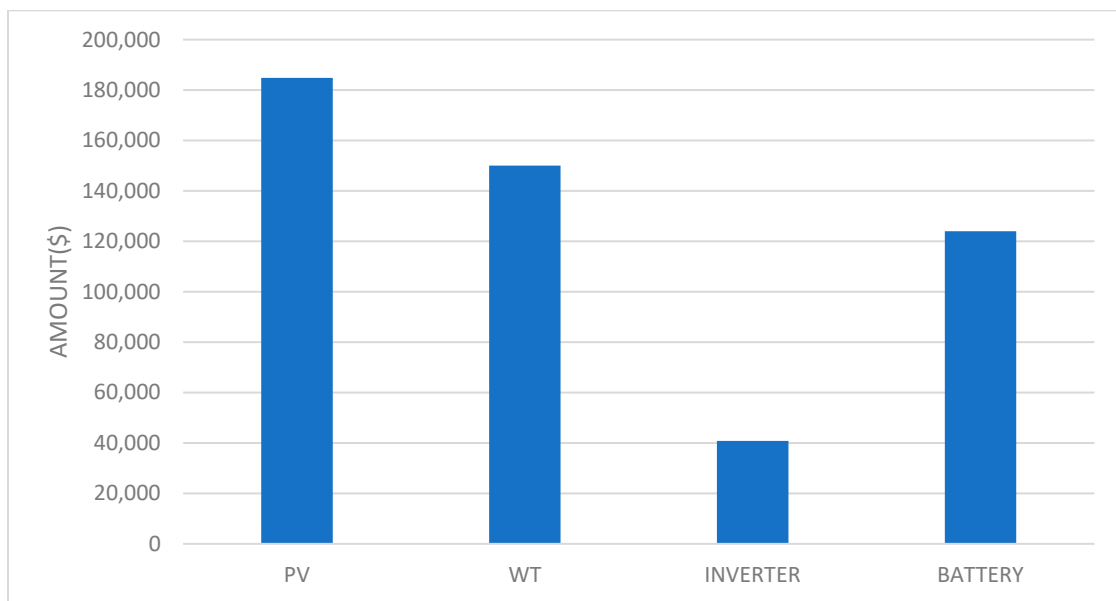
Figure 8. Breakdown of capital cost.

3.2. Result from Hybrid GA—PSO

For the Particle Swarm Optimization (PSO) algorithm, a swarm size of 4 and a maximum of 50 iterations were used. The best solution from PSO is used as the initial population for the GA. The Genetic Algorithm uses a population size of 20 and a maximum of 50 generations. After running the simulation, the result shown in Figure 9 indicates that after the fifth generation, the TAC value plateaus, indicating that further generations did not significantly improve the solution, and the optimal number of solar panels, wind turbines, inverters, and batteries that minimizes the TAC was found early. The final solution is the same as the result obtained from the PSO algorithm. This result validates the results obtained from the PSO. The power generated is shown in Figure 10.
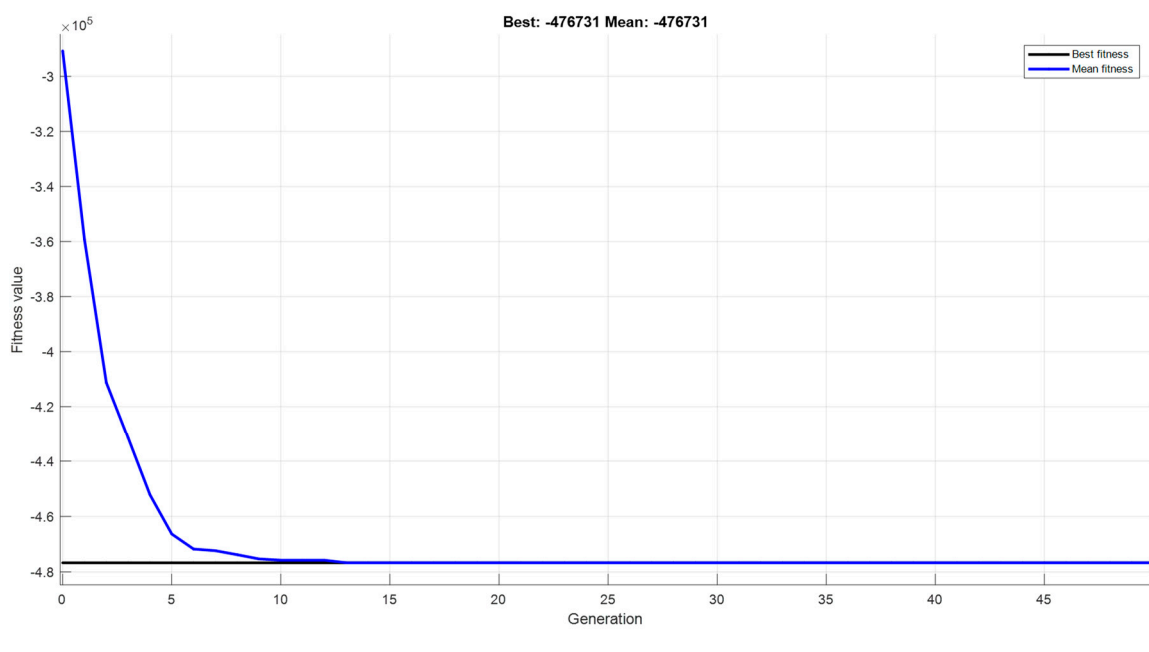
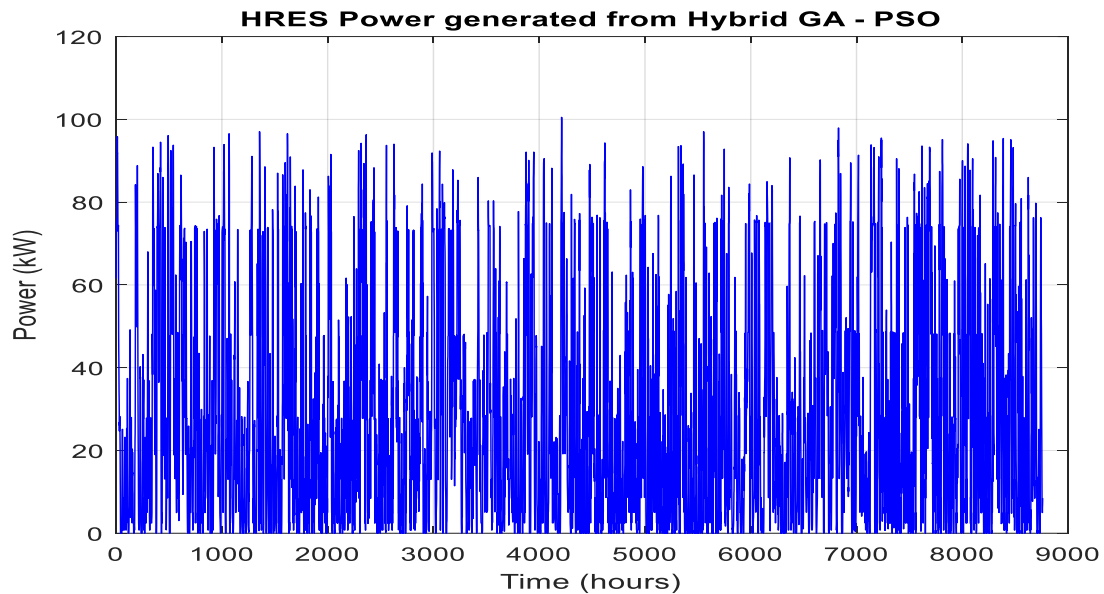**Figure 9.** Optimized fitness function from GA-PSO.

Figure 10. Power generated from the HRES for GA-PSO.

3.3. Result from NGSA-II

The multi-objective GAII uses a population size of 4 and a maximum of 150 generations. The simulation result indicates that 151, 3, 122 and 31 are the optimal sizes representing the number of solar panels, wind turbines, inverters and batteries, respectively. The TEC, TAC and LCOE are USD 469,200, USD 297,100 and 0.007/kWh, respectively. The result is shown in Figure 11. The annual electricity produced by the system was 41.79 MWh. This implies that this configuration has a deficit power of 0.38 MWh in comparison with the result obtained from the PSO and GA-PSO. In terms of the TEC, TAC and LCOE, there is a corresponding reduction of USD 7531, 4847 and 0.004/kWh, respectively, in the multi-objective GA result when compared with the other two algorithms.
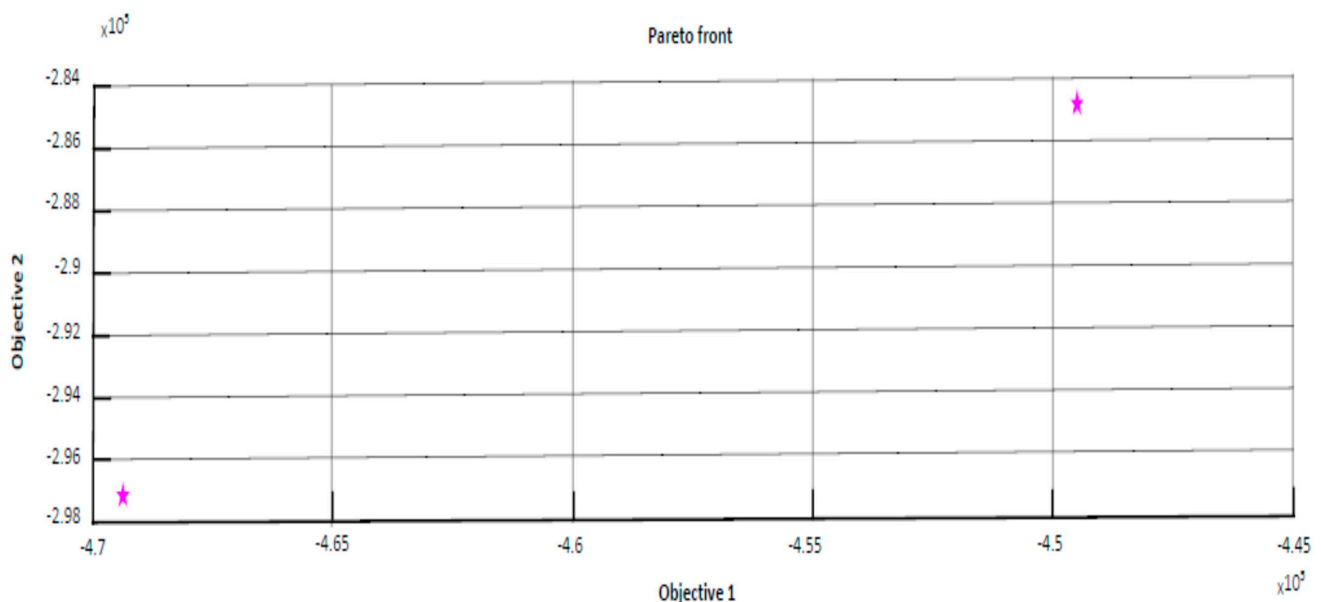

Figure 11. Pareto front from multi-objective GA.

3.4. Result from HOMER

Homer employs two different optimization algorithms. The first is a grid search algorithm that simulates all possible system configurations within the defined search space.

The newer optimizer in Homer uses a unique, derivative-free algorithm to identify the most cost-effective system. Homer then provides a list of configurations ranked by their net present cost (NPC), also known as the life-cycle cost.

Figure 12 shows the Homer model for optimization. The winning solution consists of 166 kW PV panels (Generic flat plate PV), three wind turbines (Eocycle EO25 Class III), 29 batteries (20 kW–72 kWh Primus Power Energy Cell) and 123 kW converter.
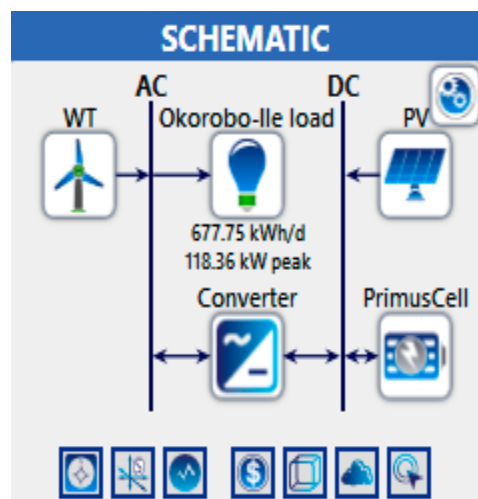

Figure 12. Homer model.

A summary of the optimal sizes is presented in Table 2. The table shows that each algorithm provides slightly different solutions, balancing costs and energy production differently. Particle Swarm Optimization (PSO) and the hybrid GA—PSO yield similar optimal configurations, while Non-dominated Sorting Genetic Algorithm II (NGSA-II) suggests slightly different component sizes. HOMER software recommends a larger PV panel capacity.

Table 2. Summary of optimal sizes.

Algorithm	PV Panels	Wind Turbines	Inverters	Batteries	TEC/NPC (USD)	LCOE (USD/kWh)
PSO	154	3	136	31	476,731 (TEC)	0.01
GA-PSO	154	3	136	31	476,731 (TEC)	0.01
NGSA-II	151	3	122	31	469,200 (TEC)	0.007
HOMER (Proprietary Derivative-free)	166	3	123	29	615,664.95 (NPC)	0.16

Cost-wise, NGSA-II achieves the lowest total cost, while HOMER's solution is costlier but provides higher energy capacity. Balancing costs and performance is crucial in designing an efficient HRES. The trade-offs are:

Cost Considerations: Lower costs are desirable, as they lead to better financial feasibility and quicker return on investment. However, excessively minimizing costs may compromise system reliability, energy production, and overall effectiveness.

Performance Considerations: High energy production and reliability are essential for meeting demand and achieving sustainability goals. Overemphasizing performance might lead to an expensive system that is not financially viable.

Given the available options, NGSA-II provides a good balance between cost and performance, with a competitive LCOE and reasonable total cost. HOMER's solution has high performance but comes at a significantly higher cost. The solution from the NGSA-II configuration is chosen due to its cost-effectiveness while maintaining satisfactory performance.

3.5. Performance Evaluation of Solution Under Various Ambient Conditions

This section details the performance analysis of energy balancing and load management. The analysis considers three weather conditions: average, poor, and good. It evaluates four specific times of the day: 06:00 h (when most residents start their day), 12:00 h (typical office hours), 18:00 h (when residents return home), and 21:00 h (bedtime). The simulation incorporates a PV array with 151 solar panels, three wind turbines, and a battery array consisting of 31 batteries.

3.5.1. CASE 1: Average Weather Condition

A usual average weather condition for the region is depicted in Figure 13. From Figure 14, the following is observed:

(**a**)

(**b**)
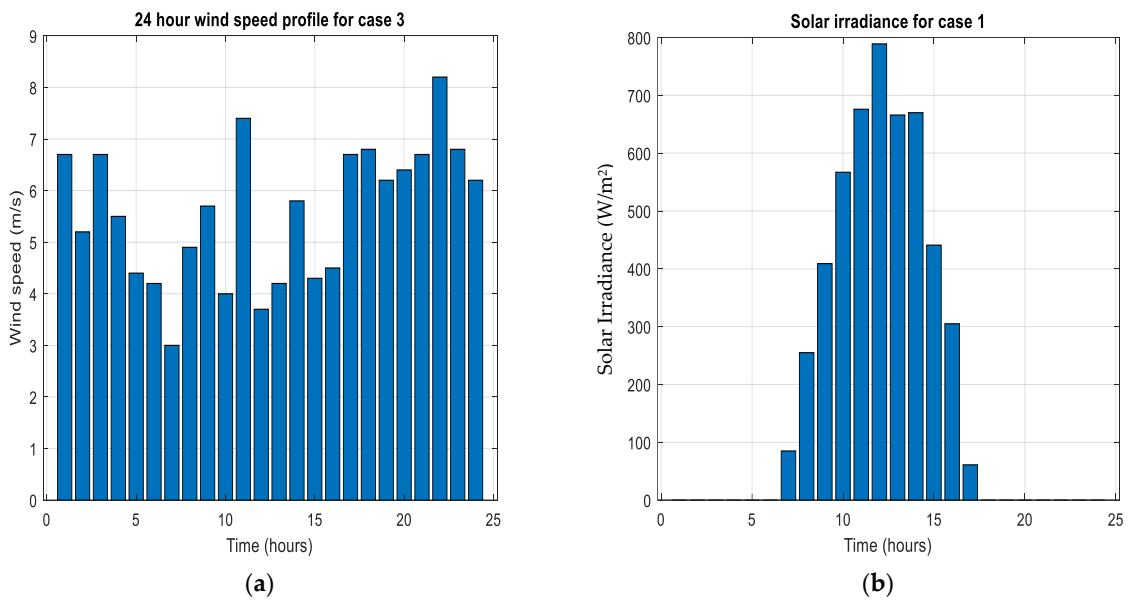
Figure 13. Average weather conditions: (**a**) wind speed at 10 m height; (**b**) solar irradiance.
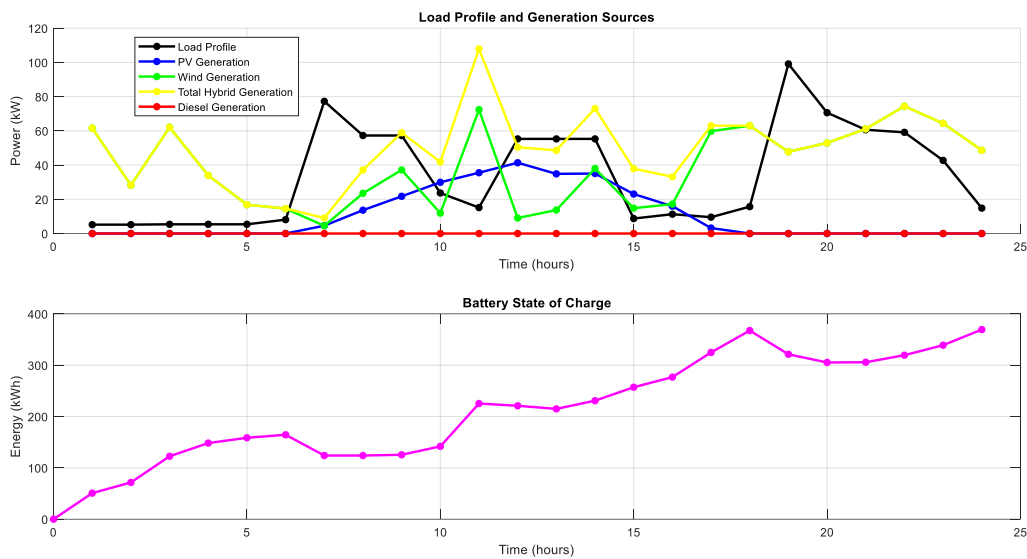

Figure 14. Case 1 performance.

At 6 h: The load demand is 77.27 kW, and the state of charge of the battery is 124 kWh. The battery is supplying power to fulfill the load demand, as the PV and wind generation are insufficient.

At 12 h: The load demand is 55.3 kW. Both solar panel and wind generation are inadequate to meet the load, so the battery, with a state of charge of 214.9 kWh, is discharging to cover the demand.

At 18 h: The load demand is 99.1 kW. Power generation from the PV is 0 kW. The wind generation is 47.77 kW and the state of charge of the battery decreases from 367.4 kWh to 321.2 kWh as it discharges to meet the load.

At 21 h: The load is 59.14 kW. PV generation remains at 0 kW, wind generation is 74.4 kW, and the battery's state of charge increases from 305.7 kWh to 319.5 kWh, indicating that the wind generation is sufficient to meet the load without discharging the battery.

3.5.2. CASE 2: Poor Weather Condition

A typical poor weather condition for the region is depicted in Figure 15. From Figure 16, the following was observed:
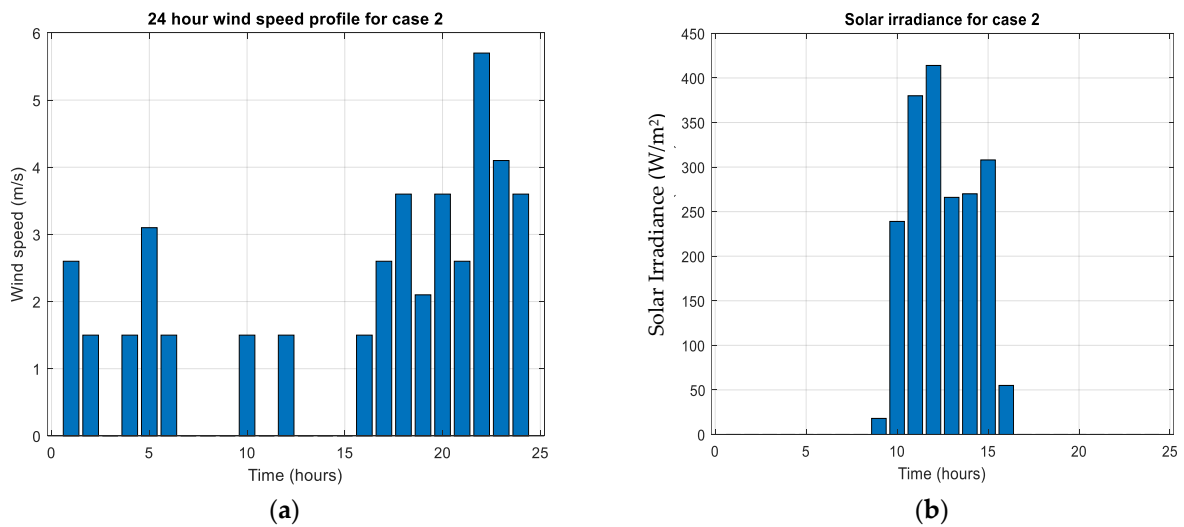

Figure 15. Poor weather conditions: (**a**) wind speed at 10 m height; (**b**) solar irradiance.
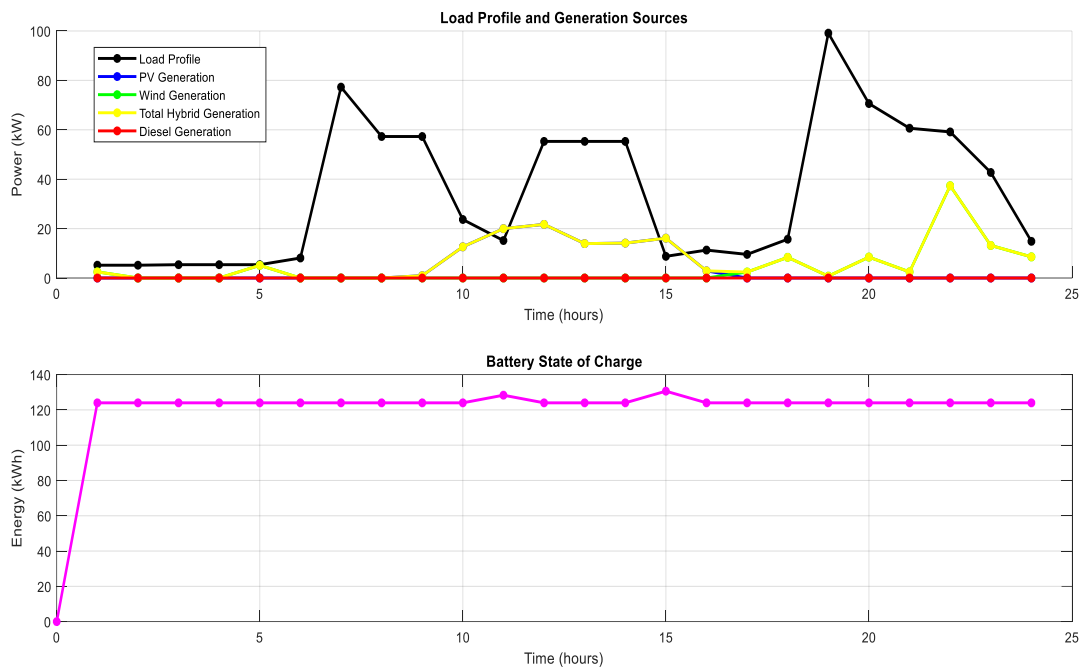

Figure 16. Case 2 performance.

At 6 h: At this time, the power generation from the PV and wind generation are minimal. The state of charge of the battery is 124 kWh, indicating that it is discharging at a high rate during this period.

At 12 h: At this time, the load demand exceeds the power generated from the PV and wind facility. The state of charge of the battery remains at 124 kWh, showing that the battery is discharging to meet the load.

At 18 and 21 h: The state of charge of the battery stays at 124 kWh, suggesting that it continues to discharge to meet the load demand.

3.5.3. CASE 3: Ideal Weather Condition

A usual ideal weather condition for the region is depicted in Figure 17. From Figure 18, the following was observed:
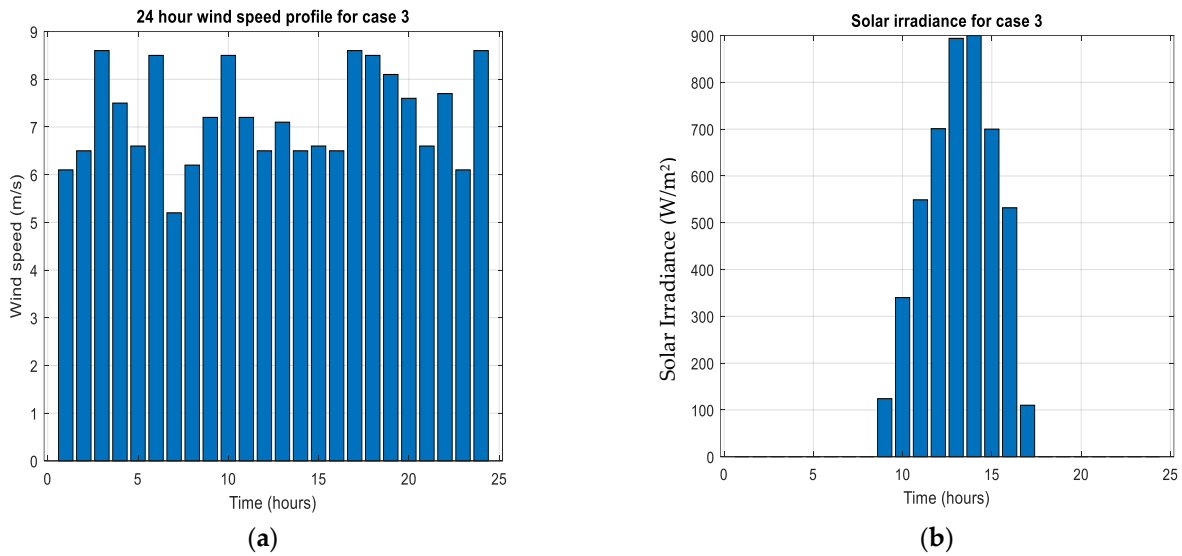

Figure 17. Good weather conditions: (**a**) wind speed at 10 m height; (**b**) solar irradiance.
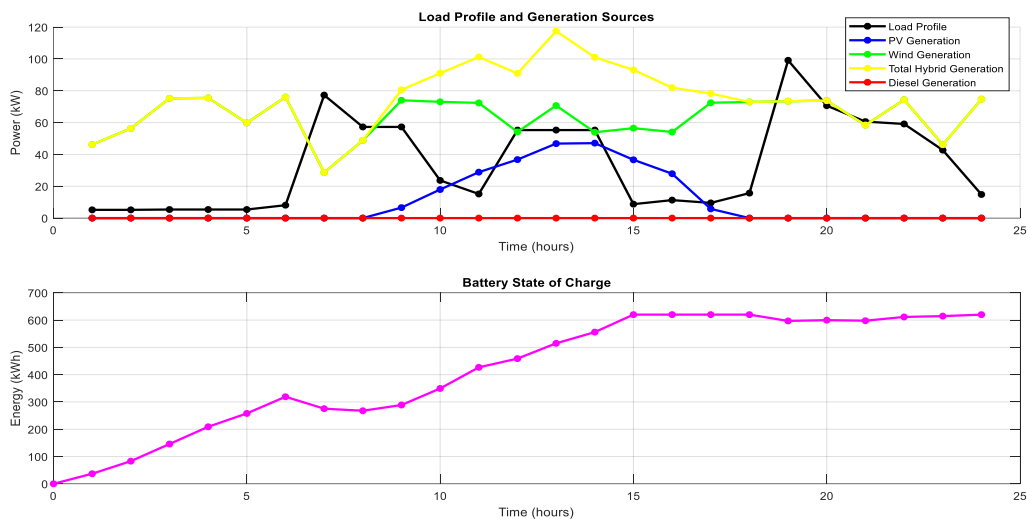

Figure 18. Case 3 performance.

At 6 h: The power generated from the PV and wind sources is 28.64 kW, which is insufficient to meet the load demand of 77.1 kW. The state of charge of the battery decreases from 319.1 kWh to 275.3 kWh, signifying that the battery is discharging to cater for the load demand.

At 12 h: At this time, there is surplus generation from the HRES, causing the battery's state of charge to increase from 458.8 kWh to 514.8 kWh as it continues to charge.

At 18 h: The power generated from the PV and wind sources cannot meet the load demand. The state of charge of the battery drops slightly from 620 kWh to 596.9 kWh, indicating that it is discharging to meet the load.

At 21 h: At this time, the power from the wind is sufficient to meet the load demand. This causes the state of charge of the battery to rise from 597.7 kWh to 611.5 kWh. The battery is not discharging, as the load demand is met by the wind generation.

Analyzing the battery's state of charge across three different weather scenarios reveals the following insights:

1. **Case 1**: The state of charge of the battery varies between 124 kWh and 367.4 kWh, demonstrating that the HRES can handle the load under typical weather conditions.
2. **Case 2**: The state of charge of the battery remains mostly stable at 124 kWh, indicating a high discharge rate due to insufficient generation from the PV and wind sources. This indicates that the system struggles to meet the load demand in these times, heavily dependent on the battery.
3. **Case 3**: The state of charge of the battery ranges from 257.3 kWh to 620 kWh. It discharges when the power from the PV and wind sources falls short of the load demand but stays fully charged when there is surplus power from the HRE system. This shows that the system efficiently manages the load under this weather condition, with the battery providing necessary backup.

Overall, this indicates that the EMS efficiently monitors and regulates the battery's state of charge under varying weather conditions.

4. Conclusions

In this study, a two-step methodology was employed to optimize and analyze a solar–wind–battery hybrid energy system for Okorobo-Ile town in Rivers State, Nigeria, using PSO. The optimization results demonstrated that the system, comprising a 151 kW PV facility, three 25 kW wind turbines, 122 kW inverters, and thirty one 20 kWh batteries, is sufficient to meet the community's energy demand. The performance of the hybrid renewable energy system varied considerably with weather conditions. Under favorable weather conditions, the PV and wind sources could meet the power demand for a greater part of the day, with excess power stored in the batteries. Conversely, in poor weather conditions, the batteries discharge frequently to cater to the power demand. This analysis underscores the critical role of weather conditions in the performance of HRE systems and highlights the necessity for efficient energy storage systems to ensure a reliable power supply under varying weather conditions.

References

1. Nigeria Electricity Production. Available online: https://www.ceicdata.com/en/indicator/nigeria/electricity-production (accessed on 14 March 2024).
2. Agajie, T.F.; Fopah-Lele, A.; Amoussou, I.; Ali, A.; Khan, B.; Tanyi, E. Optimal Design and Mathematical Modeling of Hybrid Solar PV–Biogas Generator with Energy Storage Power Generation System in Multi-Objective Function Cases. *Sustainability* **2023**, *15*, 8264. [CrossRef]
3. Adewuyi, O.B.; Shigenobu, R.; Senjyu, T.; Lotfy, M.; Howlader, A.M. Multiobjective mix generation planning considering utility-scale solar PV system and voltage stability: Nigerian case study. *Electr. Power Syst. Res.* **2019**, *168*, 269–282. [CrossRef]
4. Al-Masri, H.M.; Al-Sharqi, A.A. Technical design and optimal energy management of a hybrid photovoltaic biogas energy system using multi-objective grey wolf optimisation. *IET Renew. Power Gener.* **2020**, *14*, 2765–2778. [CrossRef]
5. Xu, L.; Ruan, X.; Mao, C.; Zhang, B.; Luo, Y. An improved optimal sizing method for wind-solar-battery hybrid power system. *IEEE Trans. Sustain. Energy* **2013**, *4*, 774–785.
6. Al-Masri, H.M.K.; Magableh, S.; Abuelrub, A.; Saadeh, O.; Ehsani, M. Impact of Different Photovoltaic Models on the Design of a Combined Solar Array and Pumped Hydro Storage System. *Appl. Sci.* **2020**, *10*, 3650. [CrossRef]
7. Nguyen, H.T.; Safder, U.; Nguyen, X.; Yoo, C. Multi-objective decision-making and optimal sizing of a hybrid renewable energy system to meet the dynamic energy demands of a wastewater treatment plant. *Energy* **2020**, *191*, 116570. [CrossRef]
8. Tian, Z.; Seifi, A.A. Reliability Analysis of Hybrid Energy System. *Int. J. Reliab. Qual. Saf. Eng.* **2014**, *21*, 1450011. [CrossRef]
9. Upadhyay, S.; Sharma, M.P. Development of hybrid energy system with cycle charging strategy using particle swarm optimization for a remote area in India. *Renew. Energy* **2015**, *77*, 586–598. [CrossRef]
10. Ma, T.; Yang, H.; Lu, L.; Peng, J. Pumped storage-based standalone photovoltaic power generation system: Modeling and techno-economic optimization. *Appl. Energy* **2015**, *137*, 649–659. [CrossRef]
11. Al-Masri, H.M.; Al-Sharqi, A.; Magableh, S.; Al-Shetwi, A.; Abdolrasol, M.; Ustun, T.S. Optimal Allocation of a Hybrid Photovoltaic Biogas Energy System Using Multi-Objective Feasibility Enhanced Particle Swarm Algorithm. *Sustainability* **2022**, *14*, 685. [CrossRef]
12. Sultan, H.M.; Menesy, A.; Kamel, S.; Korashy, A.; Almohaimeed, S.; Abdel-Akher, M. An improved artificial ecosystem optimization algorithm for optimal configuration of a hybrid PV/WT/FC energy system. *Alex. Eng. J.* **2021**, *60*, 1001–1025. [CrossRef]
13. Ukoima, K.N.; Okoro, O.I.; Obi, P.I.; Akuru, U.B.; Davidson, E. A modified multiobjective particle swarm optimization (m-mopso) for optimal sizing of a solar—Wind—Battery hybrid renewable energy system. *Sol. Compass* **2024**, *12*, 100082. [CrossRef]
14. Diab, A.A.Z.; Sultan, H.; Kuznetsov, O.N. Optimal sizing of hybrid solar/wind/hydroelectric pumped storage energy system in Egypt based on different meta-heuristic techniques. *Environ. Sci. Pollut. Res.* **2020**, *27*, 32318–32340. [CrossRef] [PubMed]
15. Alotaibi, M.A.; Eltamaly, A.M. A Smart Strategy for Sizing of Hybrid Renewable Energy System to Supply Remote Loads in Saudi Arabia. *Energies* **2021**, *14*, 7069. [CrossRef]
16. Lturki, F.A.; Awwad, E.M. Sizing and cost minimization of standalone hybrid wt/pv/biomass/pump-hydro storage-based energy systems. *Energies* **2021**, *14*, 489. [CrossRef]
17. Çetinbaş, İ.; Tamyürek, B.; Demirtaş, M. Sizing optimization and design of an autonomous AC microgrid for commercial loads using Harris Hawks Optimization algorithm. *Energy Convers. Manag.* **2021**, *245*, 114562. [CrossRef]
18. Bukar, A.L.; Tan, C.; Lau, K.Y. Optimal sizing of an autonomous photovoltaic/wind/battery/diesel generator microgrid using grasshopper optimization algorithm. *Sol. Energy* **2019**, *188*, 685–696. [CrossRef]
19. Diab, A.A.Z.; Sultan, H.; Mohamed, I.; Kuznetsov, O.; Do, T.D. Application of Different Optimization Algorithms for Optimal Sizing of PV/Wind/Diesel/Battery Storage Stand-Alone Hybrid Microgrid. *IEEE Access* **2019**, *7*, 119223–119245. [CrossRef]
20. Arasteh, A.; Alemi, P.; Beiraghi, M. Optimal allocation of photovoltaic/wind energy system in distribution network using metaheuristic algorithm. *Appl. Soft Comput.* **2021**, *109*, 107594. [CrossRef]
21. Suresh, M.; Meenakumari, R.; Panchal, H.; Priya, V.; El Agouz, E.; Israr, M. An enhanced multiobjective particle swarm optimisation algorithm for optimum utilisation of hybrid renewable energy systems. *Int. J. Ambient. Energy* **2022**, *43*, 2540–2548. [CrossRef]
22. Fadli, D.; Purwoharjono, H. Optimal sizing of PV/Diesel/battery hybrid micro-grid system using multi-objective bat algorithm. *Int. J. Eng. Sci.* **2019**, *8*, 6–14.
23. Shi, B.; Wu, W.; Yan, L. Size optimization of stand-alone PV/wind/diesel hybrid power generation systems. *J. Taiwan. Inst. Chem. Eng.* **2017**, *73*, 93–101. [CrossRef]
24. Javed, M.S.; Ma, T. Techno-economic assessment of a hybrid solar-wind-battery system with genetic algorithm. *Energy Procedia* **2019**, *158*, 6384–6392. [CrossRef]
25. Emad, D.; El-Hameed, M.; El-Fergany, A.A. Optimal techno-economic design of hybrid PV/wind system comprising battery energy storage: Case study for a remote area. Energy Convers. *Manage* **2021**, *249*, 114847. [CrossRef]
26. Hatata, A.Y.; Osman, G.; Aladl, M.M. An optimization method for sizing a solar/wind/battery hybrid power system based on the artificial immune system. *Sustain. Energy Technol. Assess.* **2018**, *27*, 83–93. [CrossRef]
27. Askarzadeh, A.; Coelho, L.S. A novel framework for optimization of a grid independent hybrid renewable energy system: A case study of Iran. *Sol. Energy* **2015**, *112*, 383–396. [CrossRef]

28. Li, J.; Liu, P.; Li, Z. Optimal design and techno-economic analysis of a solar-wind-biomass off-grid hybrid power system for remote rural electrification: A case study of west China. *Energy* **2020**, *208*, 118387. [CrossRef]

29. Goswami, A.; Sadhu, P.; Sadhu, P.K. Development of a grid connected solar-wind hybrid system with reduction in levelized tariff for a remote island in India. *J. Sol. Energy Eng.* **2020**, *142*, 044501. [CrossRef]

30. Aziz, A.S.; Tajuddin, M.; Adzman, M.; Azmi, A.; Ramli, M.A. Optimization and sensitivity analysis of standalone hybrid energy systems for rural electrification: A case study of Iraq. *Renew. Energy* **2019**, *138*, 775–792. [CrossRef]

31. Kumar, R.; Channi, H.K. A PV-Biomass off-grid hybrid renewable energy system (HRES) for rural electrification: Design, optimization and techno-economic-environmental analysis. *J. Clean. Prod.* **2022**, *349*, 131347. [CrossRef]

32. Hashem, M.; Abdel-Salam, M.; El-Mohandes, M.T.; Nayel, M.; Ebeed, M. Optimal placement and sizing of wind turbine generators and superconducting magnetic energy storages in a distribution system. *J. Energy Storage* **2021**, *38*, 102497. [CrossRef]

33. Duchaud, J.-L.; Notton, G.; Darras, C.; Voyant, C. Multi-Objective Particle Swarm optimal sizing of a renewable hybrid power plant with storage. *Renew Energy* **2018**, *131*, 1156–1167. [CrossRef]

34. Rezk, H.; Alghassab, M.; Ziedan, H.A. An Optimal Sizing of Stand-Alone Hybrid PV-Fuel Cell-Battery to Desalinate Seawater at Saudi NEOM City. *Processes* **2020**, *8*, 382. [CrossRef]

35. Donado, K.; Navarro, L.; Pardo, M. HYRES: A Multi-Objective Optimization Tool for Proper Configuration of Renewable Hybrid Energy Systems. *Energies* **2019**, *13*, 26. [CrossRef]

36. Ukoima, K.N.; Owolabi, A.B.; Yakub, A.O.; Same, N.N.; Suh, D.; Huh, J. Analysis of a Solar Hybrid Electricity Generation System for a Rural Community in River State, Nigeria. *Energies* **2023**, *16*, 3431. [CrossRef]

37. Ukoima, K.N.; Okoro, O.I.; Akuru, U.B.; Davidson, E. Technical, economic and environmental assessment and optimization of four hybrid renewable energy models for rural electrification. *Sol. Compass* **2024**, *12*, 100087. [CrossRef]

38. Dong, W.; Li, Y.; Xiang, J. Optimal sizing of a stand-alone hybrid power system based on battery/hydrogen with an improved ant colony optimization. *Energies* **2016**, *9*, 785. [CrossRef]

39. Ukoima, K.N.; Efughu, D.; Azubuike, O.C.; Akpiri, B.F. Investigating the Optimal Photovoltaic (Pv) Tilt Angle Using the Photovoltaic Geographic Information System (PVGIS). *Niger. J. Technol. (NIJOTECH)* **2024**, *43*, 101–114. [CrossRef]